

Coulomb excitation of the giant dipole resonance in light-ion inelastic scattering from ^{208}Pb

T. Izumoto, Y. -W. Lui, and D. H. Youngblood

Cyclotron Institute, Texas A&M University, College Station, Texas 77843

T. Udagawa and T. Tamura

Department of Physics, University of Texas at Austin, Austin, Texas 78712

(Received 26 May 1981)

A coupled-channel calculation including Coulomb excitation has been done for excitation of the isovector giant dipole resonance in light-ion inelastic scattering from ^{208}Pb at forward angles. It is found that the predicted cross sections for excitation of the giant dipole resonance with alpha inelastic scattering, calculated including Coulomb excitation, are much smaller than the experimental isoscalar giant monopole resonance cross section at incident energies around 100 MeV. The predicted cross section for Coulomb excitation of the giant dipole resonance increases rapidly with increasing incident energy, and the giant dipole and monopole resonance cross sections become comparable above $E_\alpha = 300$ MeV. For inelastic scattering of ^3He , deuterons, and protons at forward angles, Coulomb excitation of the giant dipole resonance is found to be comparable to the giant monopole resonance cross section at $100 < E^{\text{lab}} < 200$ MeV. Coulomb excitation of the giant dipole resonance is strongly inhibited by momentum mismatch between incident and outgoing waves due to the large negative Q values. This mismatch is reduced for lighter projectile masses and higher incident energies. As the giant monopole and dipole resonances are almost coincident, giant dipole resonance excitation must be properly accounted for in studies of the giant monopole resonance.

[NUCLEAR REACTIONS Coupled-channel calculation of $\sigma(\theta)$; for
Coulomb excitation of isovector dipole resonance in ^{208}Pb ; from (α, α') ,
 $(^3\text{He}, ^3\text{He}')$, (d, d') , and (p, p') scattering.]

I. INTRODUCTION

The isoscalar giant monopole resonance (GMR) in nuclei has been established by inelastic alpha scattering measurements.¹ Presently, all of the experimental evidence of the GMR come from inelastic scattering of various light ions with high incident energy (of 80–220 MeV). These measurements have generally been done at forward scattering angles in order to distinguish the GMR from the giant quadrupole resonance (GQR). As the GMR is almost coincident with the isovector giant dipole resonance (GDR) in excitation energy, it is important to theoretically investigate to what extent the GDR is excited.

Though nuclear excitation of the GDR is usually weak, Coulomb excitation can be significant at forward angles. An estimate² with the plane-wave

Born approximation (PWBA) suggests that the Coulomb excitation cross section of the GDR is comparable to the measured cross section of the GMR, and that their angular distribution may be similar at forward angles. For a fixed incident energy, the cross section for Coulomb excitation is further predicted to be proportional to mz^2 , where m and z are the mass and charge number of the projectile. Therefore, the effect of Coulomb excitation may be more pronounced in inelastic alpha scattering than in proton, deuteron, or ^3He scattering. A study³ with the distorted-wave Born approximation (DWBA) was reported very recently which indicated Coulomb excitation of the GDR should be significant in ^3He and proton studies of the GMR which have been carried out.

The primary aim of the present study was to assess the contribution from Coulomb excitation of

the GDR in the region of the GMR in ^{208}Pb in (α, α') scattering with incident energies between 96 and 218 MeV.³⁻⁵ There is a serious momentum mismatch in the excitation of such low spin states having large negative Q values (~ 13 MeV). Distortion effects on incident and outgoing waves may play a decisive role in such a case and the simple mz^2 dependence of Coulomb excitation as predicted by the PWBA does not survive in distorted-wave calculations.

Calculations including Coulomb excitation must meet the following two requirements: (1) Large wave numbers of 3 to 7 fm^{-1} require a small step size for the radial integration. (2) The long range nature of the Coulomb form factor requires that the integration should be performed to a distant point from the origin to get convergence. A coupled-channel (CC) program, JPWKB, by Kim *et al.*⁶ was employed to perform fast calculations meeting these requirements without losing much accuracy. Calculations were also performed for inelastic scattering of other projectiles exciting the GDR in ^{208}Pb . Specific calculations were carried out for projectiles used in recently published studies on the excitation of the GMR with 201 MeV protons,³ 86 and 108 MeV deuterons,^{3,5} and 108.5 MeV ^3He particles.⁷

In Sec. II, we give a brief account of the method of the CC calculations. In Sec. III, the results of numerical analysis are presented for the GMR and GDR in ^{208}Pb excited by inelastic scattering of various light ions. A summary is given in Sec. IV.

II. METHOD OF CALCULATIONS

In the present CC study of inelastic scattering, use is made of a computer program JPWKB, developed some time ago by Kim *et al.*⁶ We thus describe briefly the method used in the program.

The radial region is divided into two parts separated by a separation distance R_s , as shown in Fig. 1. The first is the internal region ($0 < r \leq R_s$), where both nuclear and Coulomb excitation are important. The CC equations are solved exactly, and the program JUPITER-1^{8,9} is used in its original form to generate N sets of independent solutions $[v_{pq}(r); p = 1, 2, \dots, N]$. The second is the external region ($r > R_s$), where only the Coulomb interaction has to be considered. The CC equations are, however, solved approximately by using a Wentzel-Kramers-Brillouin (WKB)-type of approximation originally introduced by Alder and Pau-
li.^{10,11}

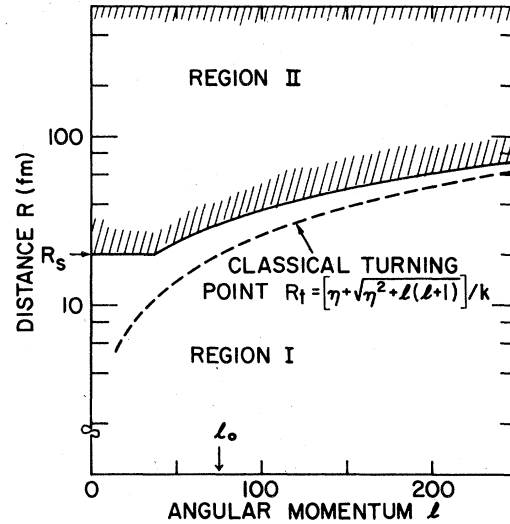


FIG. 1. Division of the radial integration region in solving CC equations.

Since detailed descriptions of the internal solutions were given earlier,^{8,9} we limit our discussion to the external solution of the CC equations and the matching condition at $r = R_s$. The expression of the S matrix may be written as

$$S = U^T S^{(1)} U. \quad (2.1)$$

Here a unitary transformation U contains all the effect of Coulomb excitation in the external region. The internal S -matrix $S^{(1)}$ is obtained by matching smoothly the two sets of N independent solutions obtained for each partial wave at $r = R_s$.

In the external region, the radial part of the wave function in the channel q is given as

$$u_q(r) = \frac{1}{\sqrt{k_q}} [h_q^{(-)}(r) a_q^{(-)}(r) - h_q^{(+)}(r) a_q^{(+)}(r)], \quad (2.2)$$

with

$$h_q^{(\pm)}(r) = G_l(k_q r) \pm i F_l(k_q r), \quad (2.3)$$

where k_q is the wave number. F_l and G_l are the regular and irregular Coulomb wave functions, respectively. We neglect the spin-orbit interaction in the optical potential. Thus, the channel index q can be specified by the spin I_n of the state $|n\rangle$ of the target nucleus, the orbital angular momentum l , and the total angular momentum of the system $\vec{J} = \vec{I}_n + \vec{l}$.

The CC equation for the unknown functions $a_q^{(\pm)}(r)$ is obtained by inserting Eq. (2.2) into the exact CC equation for $u_q(r)$ [see Eq. (25) of Ref. 8] and multiplying by either $h_q^{(+)}(r)$ or $h_q^{(-)}(r)$ from the left hand side. We further introduce the following three approximations: (i) $h_q^{(\pm)}(r)$ are approximated by those obtained by the WKB method. (ii) The second derivative of $a_q^{(\pm)}(r)$ with respect to r is neglected. (iii) The rapidly oscillating terms like $h_q^{(+)}(r)h_{q'}^{(+)}(r)$ and $h_q^{(-)}(r)h_{q'}^{(-)}(r)$ are neglected. One can see that $a_q^{(\pm)}(r)$ satisfies¹⁰

$$\phi_q = k_q r / p_q^2 + \eta_q \log \left[\sqrt{\eta_q^2 + l(l+1)} / (k_q r - \eta_q + \sqrt{k_q r / p_q^2}) \right] - \sqrt{l(l+1)} \cos^{-1} \left\{ [\eta_q k_q r + l(l+1)] / k_q r \sqrt{\eta_q^2 + l(l+1)} \right\}, \quad (2.7)$$

with η_q being the Sommerfeld parameter. $v_{qq'}^J$ in Eq. (2.5) is exactly the same as the interaction matrix element given by Eq. (27) of Ref. 8, except that no nuclear interaction is involved in Eq. (2.5).

Note that $a^{(\pm)}(r)$ are not independent but are related through

$$a_q^{(-)*}(r) = a_q^{(+)}(r). \quad (2.8)$$

This may be seen if one notices that $v_{qq'}^{(\pm)}$ satisfies the symmetry relation

$$v_{qq'}^{(+)*} = \mp v_{qq'}^{(+)} . \quad (2.9)$$

Now let us denote N independent sets of solutions of Eq. (2.4) by $[a_{kq}^{(+)}(r); k=1,2,\dots,N]$, which are obtained by setting the boundary condition at $r=R_s$ as

$$a_{kq}^{(\pm)}(r=R_s) = \delta_{kq} . \quad (2.10)$$

This normalization guarantees that $a_{kq}^{(\pm)}(r)$ are unitary matrices.

The solution $u_{qq_0}(r)$ in the external region may be given in the form

$$u_{qq_0} = \frac{1}{\sqrt{k_q}} \sum_k \left[h_q^{(-)}(r) a_{kq}^{(-)}(r) \alpha_{kq_0}^{(-)} - h_q^{(+)}(r) a_{kq}^{(+)}(r) \alpha_{kq_0}^{(+)} \right]. \quad (2.11)$$

From the boundary condition that $u_{qq_0}(r)$ takes the asymptotic form

$$u_{qq_0}(r) \rightarrow \frac{1}{\sqrt{k_q}} [h_q^{(-)}(r) \delta_{qq_0} - h_q^{(+)}(r) S_{qq_0}], \quad (2.12)$$

one can obtain

$$I = a^{(-)}(r=\infty) \alpha^{(-)} \quad (2.13)$$

and

$$S = a^{(+)}(r=\infty) \alpha^{(+)} . \quad (2.14)$$

$$\frac{da_q^{(\pm)}(r)}{dr} = \mp \sum_{q'} v_{qq'}^{(\pm)} a_{q'}^{(\pm)}(r), \quad (2.4)$$

where

$$v_{qq'}^{(+)} = \frac{1}{2i} \frac{p_q p_{q'}}{\sqrt{k_q k_{q'}}} v_{qq'}^J e^{\pm i(\phi_q - \phi_{q'})}, \quad (2.5)$$

$$p_q = \{ 1 - (2\eta_q / k_q r) - [l(l+1) / k_q^2 r^2] \}^{-1/4}, \quad (2.6)$$

and

The unknown matrix $\alpha^{(+)}$ is determined by the requirement that the external solutions (2.11) should be matched at $r=R_s$ smoothly to the internal solutions:

$$u_{qq_0}(r) = \frac{1}{\sqrt{k_q}} \sum_p v_{pq}(r) b_{pq_0}, \quad (2.15)$$

where coefficients b_{pq_0} are also to be determined.

The S matrix is thus completely determined. It is interesting to note that Eq. (2.14) can be rewritten as

$$S = a^{(+)}(r=\infty) S^{(1)} a^{(-)}(r=\infty), \quad (2.16)$$

with

$$S^{(1)} = \alpha^{(+)} [\alpha^{(-)}]^{-1}, \quad (2.17)$$

which is the same form as given in Eq. (2.1).

Comparing Eq. (2.16) with Eq. (2.1), we obtain the matrix U as

$$U = [a^{(-)}(r=\infty)]^{-1}. \quad (2.18)$$

Since the first derivative of $a_{kq}^{(\pm)}(r)$ is very small already at $r=R_s$, it is easily seen from the matching equations that the internal S matrix $S^{(1)}$ can be replaced to a good approximation by the S matrix obtained from the original JUPITER-1. Kim *et al.*⁶ assumed this replacement. We used the S matrix given in Eq. (2.14) in the present calculation.

Introducing the C matrix as

$$C = \frac{1}{2i} (I - S), \quad (2.19)$$

the cross section can be expressed as

$$\frac{d\sigma}{d\Omega} = \frac{1}{2I_0 + 1} \sum_{M_n M_0} |X_{M_n M_0}(\theta)|^2. \quad (2.20)$$

X is given in terms of the C matrix introduced above as

$$X_{M_n M_0}(\theta) = \sum_{l'l'} \frac{4\pi}{\sqrt{k_q k_{q_0}}} \hat{l} \hat{l}' e^{i(\sigma_l^{(n)} + \sigma_l^{(0)})} \\ \times \langle l'l_0 M_0 | J M_0 \rangle \langle l'l_n M_l M_n | J M_0 \rangle C_{l'l_n l_0}^J Y_{l'M_l}(\theta). \quad (2.21)$$

It should be remembered that the CC equation for $a_q^{(\pm)}(r)$ given by Eq. (2.4) can be solved with a large step size, since all functions involved are very smooth functions of r . This significantly speeds up the computation. In order to save more computer time, an interpolation is used to generate C matrices for higher partial waves for which only the Coulomb excitation effect is important. The integration of the CC equations is made of all the l values up to a certain l value, say l_0 . Beyond l_0 the integration is carried out with a step of $\Delta l = 10$ and the C matrices for the l values in between are generated by the four-point interpolation method.

III. NUMERICAL RESULTS

A. (α, α') scattering

We first discuss Coulomb and nuclear excitation of the GDR in ^{208}Pb in terms of the CC method. In the calculations, the GDR is assumed to exhaust the full value (100%) of the energy-weighted sum rule (EWSR) obtained using a radius parameter $r_0 = 1.25$ fm. The complex form factor for nuclear excitation is obtained by following the prescription given by Satchler.¹² The optical potential parameters used in the calculation have been taken from Refs. 5, 13, and 14, and are listed

in Table I. In the calculations the internal region of radial integration extends up to 10 fm beyond the classical turning point. The maximum radius R_{max} of the external region was 600 fm, which is large enough to obtain convergence of S -matrix elements for angular momenta up to $250\hbar$. In order to demonstrate this, an S -matrix element $S_{l-1,l}^{J=l}$ for values of R_{max} up to 600 fm is plotted in Fig. 2. The other matrix element $S_{l+1,l}^{J=l}$ is much smaller than the above one, and is not given here. We intend to determine the angular distributions of the GDR down to $\theta = 1 - 2^\circ$. For cases of high incident energies (≥ 200 MeV), partial waves up to $250\hbar$ are adequate as can be understood from the classical angle of deflection, $\theta = 2\eta/l_{\text{max}}$. For lower incident energies, we do not need to include very high partial waves, since the magnitude of the S -matrix element falls off very rapidly because of large momentum mismatch (as will be discussed later).

The calculated cross sections of the GDR (dashed-dotted lines) for incident energies of 96, 129, 172, and 218 MeV are shown in Fig. 3. At the lowest energy, $E_\alpha = 96$ MeV, the cross section of the GDR is dominated by nuclear excitation, and there is destructive interference between Coulomb and nuclear excitation. As the incident energy increases, both contributions increase. Coulomb excitation, however, increases more rap-

TABLE I. Optical potential parameters used in the calculation.

	E^{lab} (MeV)	V (MeV)	r (fm)	a (fm)	W (MeV)	r_w (fm)	a_w (fm)	r_c (fm)
Alpha	96	89.3	1.35	0.71	52.7	1.35	0.71	1.30
	129	89.3	1.35	0.71	52.7	1.35	0.71	1.30
	172	155.0	1.282	0.677	23.26	1.478	0.733	1.30
	218	119.9	1.26	0.74	21.3	1.45	0.80	1.30
^3He	108.5	115.0	1.182	0.857	17.2	1.551	0.769	1.30
	217	78	1.25	0.86	24.1	1.43	0.81	1.30
d	86	83.74	1.15	0.817	17.84 ^a	1.028	1.24	1.30
	108	99	1.05	0.98	25.5 ^a	1.206	0.75	1.30
p	201	12.11	1.238	0.836	18.58	1.232	0.642	1.18

^aSurface absorption is assumed.

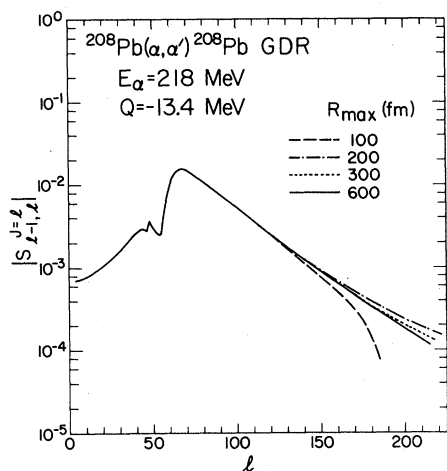


FIG. 2. Absolute value of an S -matrix element $|S_{l-1,l}^{J=1}|$ for the GDR excitation for $E_\alpha = 218$ MeV. The radial integration range is varied from 100 to 600 fm.

idly than nuclear excitation does. At the highest energy, $E_\alpha = 218$ MeV, Coulomb excitation dominates nuclear excitation by a factor of 3. The energy dependence of these contributions at forward angles is a result of the large momentum mismatch involved. This can be seen from the difference between the incident and outgoing momenta:

$$hq = \hbar |k_i - k_f| \approx Q / \sqrt{2E^{c.m.}/m}, \quad (3.1)$$

where Q is the reaction Q value, m is the reduced mass of the system, and $E^{c.m.}$ is the incident energy in the center-of-mass system. This mismatch introduces oscillations in the integrand in the interaction matrix elements, and reduces the resultant values of the matrix elements. This explains why both of the contributions increase with decreasing q (or increasing $E^{c.m.}$). The reduction due to this mismatch is expected to be stronger for the long range Coulomb interaction than the short-range nuclear interaction. (We may alternatively discuss the Fourier components of both interactions in momentum space.) This explains also why Coulomb excitation increases more rapidly than nuclear excitation with increasing $E^{c.m.}$ (or decreasing q). Note that the effect of momentum mismatch can also be checked by varying the reaction Q value artificially. This is illustrated in Fig. 4, where absolute values of the S -matrix element $|S_{l-1,l}^{J=1}|$ for $E_\alpha = 96$ MeV are plotted as a function of the angular momentum l . We see that for increasing $|Q|$ [or increasing q in Eq. (3.1)], the S -matrix element for high partial waves falls off and becomes less significant.

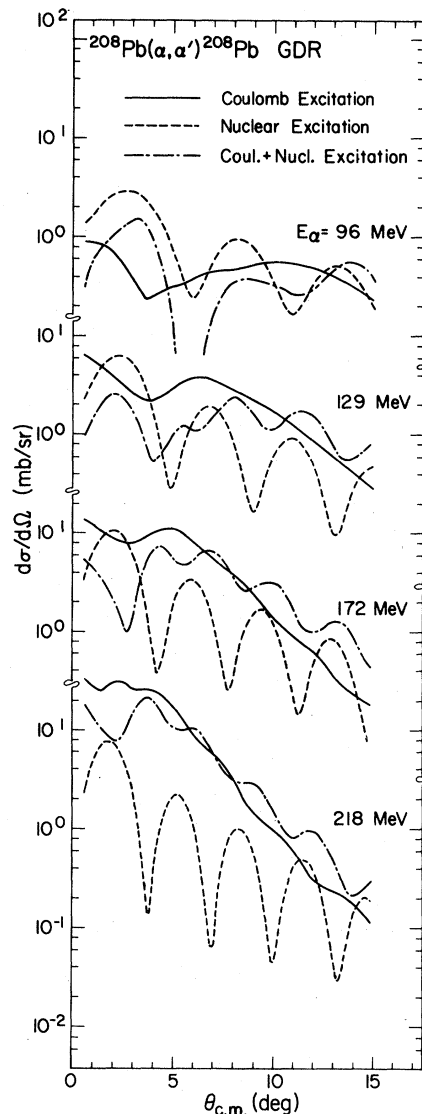


FIG. 3. Theoretical prediction of excitation cross sections of the GDR in ^{208}Pb from inelastic alpha scattering (dashed-dotted lines). The individual contributions from Coulomb and nuclear excitations are shown by solid and dashed lines, respectively.

In Fig. 5, calculated cross sections of the GMR and the GDR are compared with the experimental data.³⁻⁵ For the GMR, the form factor (version 1) from Ref. 15 was assumed and the EWSR was evaluated by using the radius of the imaginary part of the optical potential for the radius parameter. The calculated cross sections of the GMR agree quantitatively with results³⁻⁵ obtained by the DWBA. However, the DWBA results in Ref. 3 for Coulomb excitation of the GDR could not be reproduced, which might suffer from inadequacy of

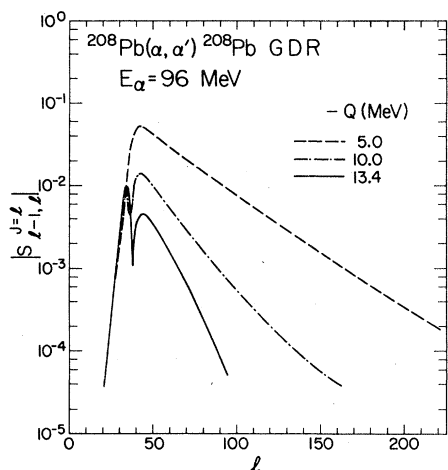


FIG. 4. Absolute value of an S -matrix element $|S_{l-1,l}^{j=l}|$ for the GDR excitation for $E_\alpha=96$ MeV. The reaction Q value is varied from $Q = -13.4$ MeV to -5.0 MeV.

the conventional integration method. For the lower incident energies, calculated GDR cross sections (σ_D) are negligibly small compared with those of the GMR (σ_M) and the experimental data. However, as the incident energy becomes higher, σ_D becomes almost comparable to σ_M . Such a rapid growth of σ_D as compared with σ_M results mainly from the rapid increase of Coulomb excitation of the GDR. This trend continues as the incident energy is raised. At $E_\alpha=320$ MeV, σ_D is predicted to be comparable to σ_M at forward angles. It is concluded that the effect of Coulomb excitation of the GDR cannot be neglected at such energies. This result disagrees with a speculation based on DWBA analysis in Ref. 3.

B. Inelastic scattering of other light ions

Similar analyses have been made for inelastic scattering of ^3He particles, deuterons, and protons from the GMR and the GDR in ^{208}Pb . The cross sections for inelastic scattering of ^3He particles are shown in Fig. 6 for $E(^3\text{He}) = 108.5$ MeV (Ref. 7) and 217 MeV obtained using the optical potential parameters from Refs. 16 and 17, respectively. The contributions of the nuclear interaction to excitation of the GDR are not included in the figure because of uncertainty in the strength of the isovector coupling potential. For 108.5 MeV, the Goldhaber-Teller model (without Coulomb excitation) predicts a maximum cross section of ~ 0.4 mb/sr at 3° with use of the real coupling potential $v_1=39$ MeV taken from Ref. 18. This is much

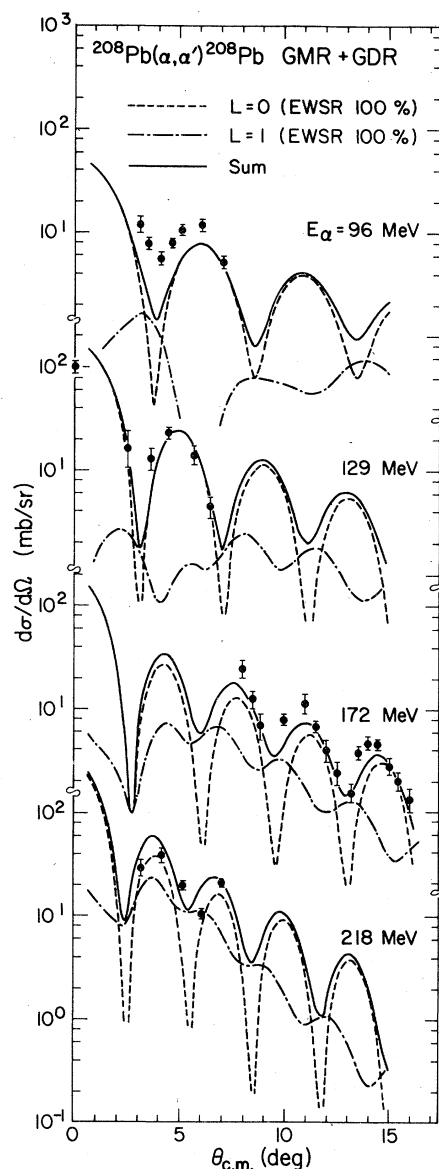


FIG. 5. Excitation of the 13.4 MeV peak in ^{208}Pb from alpha inelastic scattering is compared with theoretical estimates. The experimental data are taken from Refs. 3–5.

smaller than the Coulomb excitation cross section.

The GMR in ^{208}Pb has also been observed in inelastic scattering of deuterons at $E_d=86$ MeV⁵ and 108 MeV⁷. We note that the experimental cross section at 108 MeV has been renormalized in Ref. 3 to be smaller by a factor of 3 than the previously published value.¹⁹ CC predictions are given in Fig. 7 in comparison with the experimental data. The estimated cross section of GDR is appreciable at angles below 5° compared to the GMR

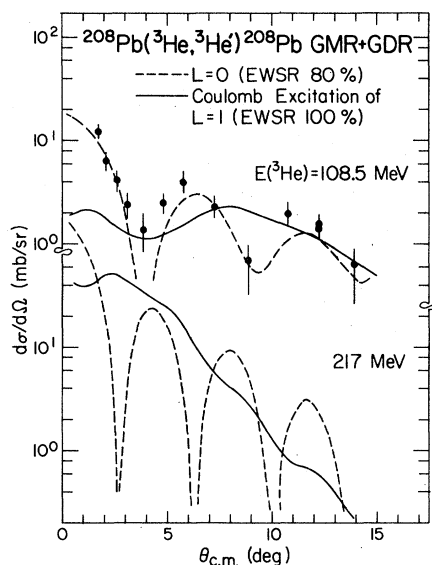


FIG. 6. Inelastic scattering of ${}^3\text{He}$ particles from the GMR region in ${}^{208}\text{Pb}$ at $E({}^3\text{He}) = 108.5$ MeV and theoretical estimates for 108.5 and 217 MeV. The data are taken from Ref. 7.

cross section. The EWSR limit for the GDR and the GMR have been evaluated by using the radius parameter $r_0 = 1.25$ fm here and in the proton case.

The results of a CC calculation for GMR and GDR excitation in proton scattering are shown in Fig. 8 in comparison with the experimental data.³ The optical potential parameters were taken from Ref. 20. Coulomb excitation of the GDR dominates the cross section at forward angles, which agrees with the DWBA analyses given earlier.^{3,21}

It is interesting to compare Coulomb excitation induced by protons and alphas (or ${}^3\text{He}$ particles) with almost the same incident energy of 200 MeV. See Fig. 8 and the bottom of Fig. 2 (or 6). The latter cross section is quite comparable to the former, which contradicts the mz^2 dependence of the PWBA.² It is worthwhile to remember that momentum mismatch in Eq. (3.1) becomes of less importance for projectiles with smaller masses. We may thus conclude that the enhancement effect due to a reduction of momentum mismatch for small projectiles dominates the mz^2 dependence of the cross section.

IV. SUMMARY

A CC calculation has been done for excitation of the GMR and GDR in ${}^{208}\text{Pb}$ from the inelastic scattering of light ions. Special emphasis was

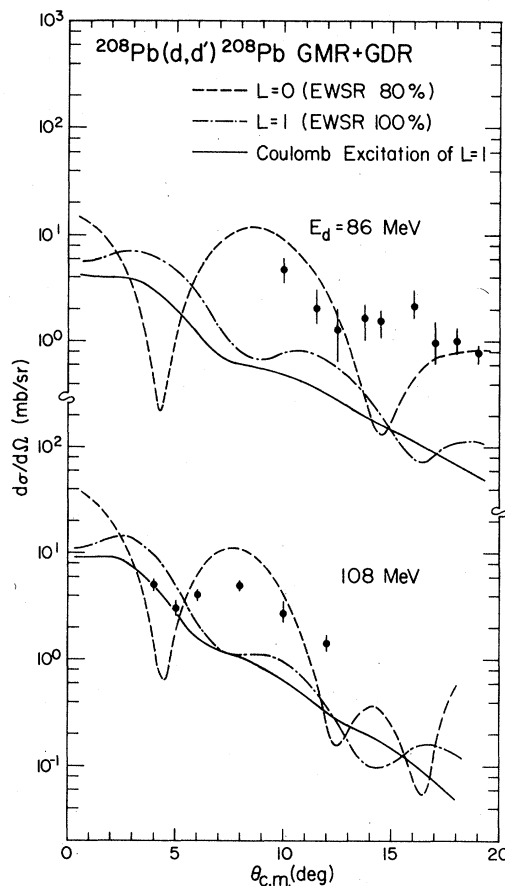


FIG. 7. Inelastic scattering of deuterons from the GMR region in ${}^{208}\text{Pb}$ at $E_d = 86$ and 108 MeV and theoretical estimates. The data are taken from Refs. 3 and 5.

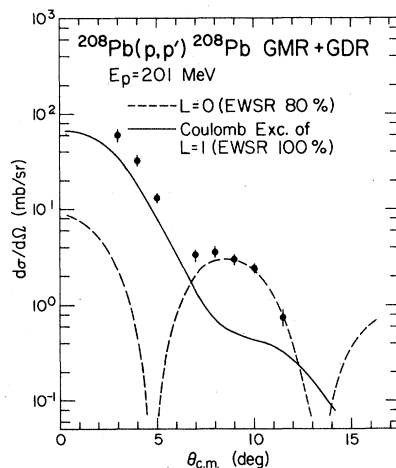


FIG. 8. Inelastic scattering of protons from the GMR region in ${}^{208}\text{Pb}$ at $E_p = 201$ MeV and theoretical estimates. The data are taken from Ref. 3.

given to computing Coulomb excitation of the GDR, which might suffer from difficulties with conventional CC and DWBA programs for light-ion reactions. A large range of radial integration (up to a few hundred fm) and a small step size are required because of a slow damping of the radial form factor and large wave numbers, respectively. Contributions from high partial waves must be summed up accurately to set the cross sections at forward angles, which are important in comparing with experimental data. These requirements have been fulfilled by making use of a program JPWKB²². We note that similar approaches^{23,24} have also been reported using the factorization (2.2) proposed by Alder and Pauli.^{10,11}

The CC calculation of the GMR and GDR in ²⁰⁸Pb revealed some interesting features. For alpha inelastic scattering of 96 and 129 MeV, the Coulomb excitation cross section of the GDR is found to be far less than the experimental cross sections of the GMR, which supports the DWBA analyses^{1,4} and contradicts an estimate in terms of the PWBA with a radial cutoff.² However, as the incident energy goes higher, say $E_\alpha = 320$ MeV, an appreciable contribution comes from Coulomb excitation of the GDR to the observed giant resonances at 13.4 MeV.

Our results differ from a conclusion drawn in Ref. 3, which may suffer from numerical inaccuracy of the DWBA calculation. We, however, note that a linearity of the calculated cross section versus the square of the coupling strength is observed in the CC calculation, which implies the validity of the DWBA in these applications. For inelastic scattering of other light projectiles, Coulomb excitation of the GDR may not be neglected even at low incident energy ~ 100 MeV, and its cross sections are found to grow with increasing incident energy. The observed energy and projectile-mass dependence of the cross section are well explained in terms of momentum mismatch involved, which is serious especially for larger projectiles with lower incident energy. The same conclusion drawn above may also apply to medium-mass nuclei, where the systematics of the GMR have been recently disclosed by alpha inelastic scattering.⁴

This work was supported by the U. S. Department of Energy under Contract Nos. DE-AS05-80ER10565 and DE-AS05-81ER40031, and by the National Science Foundation and the Robert A. Welch Foundation.

¹D. H. Youngblood, C. M. Rozsa, J. M. Moss, D. R. Brown, and J. D. Bronson, *Phys. Rev. Lett.* **39**, 1188 (1977).

²M. Kawai and T. Terasawa, in *Proceeding of the International Symposium on Highly Excited States*, edited by H. Ikegami and M. Muraoka (Osaka University, Japan, 1980), p. 371; M. Kawai and T. Terasawa, *Prog. Theor. Phys.* **22**, 513 (1959).

³C. Djalali, N. Marty, M. Morlet, A. Willis, V. Comparat, and R. Frascaria, *Z. Phys. A* **298**, 79 (1980).

⁴D. H. Youngblood, P. Bogucki, J. D. Bronson, U. Garg, Y. -W. Lui, and C. M. Rozsa, *Phys. Rev. C* **23**, 1997 (1981).

⁵H. P. Morsch, C. Sükösd, M. Rogge, P. Turek, H. Machner, and C. Mayer-Böricke, *Phys. Rev. C* **22**, 489 (1980).

⁶B. T. Kim, T. Udagawa, D. H. Feng, and T. Tamura, Fortran program JPWKB (unpublished).

⁷M. Buenerd, C. Bonhomme, D. Lebrun, P. Martin, J. Chauvin, G. Duhamel, G. Perrin, and P. de Saintignon, *Phys. Lett.* **84B**, 305 (1979).

⁸T. Tamura, *Rev. Mod. Phys.* **37**, 679 (1965).

⁹T. Tamura, Oak Ridge National Laboratory Report ORNL-4152, 1967.

¹⁰K. Alder and H. K. A. Pauli, *Nucl. Phys. A* **128**, 193

(1969).

¹¹F. Rösel, J. X. Saladin, and K. Alder, *Comput. Phys. Commun.* **8**, 35 (1974).

¹²G. R. Satchler, *Nucl. Phys. A* **195**, 1 (1972).

¹³D. H. Youngblood, J. M. Moss, C. M. Rozsa, J. D. Bronson, A. D. Bacher, and D. R. Brown, *Phys. Rev. C* **13**, 994 (1976).

¹⁴L. Bimbot, B. Tatischeff, I. Brissaud, Y. LeBornec, N. Frascaria, and A. Willis, *Nucl. Phys. A* **210**, 397 (1973).

¹⁵G. R. Satchler, *Part. Nucl.* **5**, 105 (1973).

¹⁶A. Djaloeis, J. D. Didelez, A. Galonsky, and W. Oelert, *IKP Annual Report 1977* (KFA, Jülich), p. 2.

¹⁷N. Willis, I. Brissaud, Y. Lebornec, B. Tatischeff, and G. Duhamel, *Nucl. Phys. A* **204**, 454 (1973).

¹⁸G. R. Satchler, in *Isospin in Nuclear Physics*, edited by D. H. Wilkinson (North-Holland, Amsterdam, 1969).

¹⁹A. Willis, M. Morlet, N. Marty, R. Frascaria, C. Djalali, V. Comparat, and P. Kitching, *Nucl. Phys. A* **344**, 137 (1980).

²⁰W. T. H. Van Oers, H. Haw, N. E. Davison, A. Ingemarsson, F. Fagerstrom, and G. Tibell, *Phys. Rev. C* **10**, 307 (1971).

²¹F. E. Bertrand, in *Common Problems in Low-and*

- Medium-Energy Nuclear Physics*, edited by B. Castel, B. Goulard, and F. C. Khanna (Plenum, New York, 1979), p. 417.
- ²²Its application to inelastic scattering of heavy ions results in reasonable agreement with the published results (Ref. 25) obtained by using the program ECIS by J. Raynal.
- ²³M. Ichimura, M. Igarashi, S. Landowne, C. H. Dasso, B. S. Nilsson, R. A. Broglia, and A. Winter, *Phys. Lett* **67B**, 129 (1977).
- ²⁴M. Rhoades-Brown, M. H. Macfarlane, and S. C. Pieper, *Phys. Rev. C* **21**, 2417 (1980).
- ²⁵M. E. Coberm, N. Lisbona, and M. C. Mermaz, *Phys. Rev. C* **13**, 674 (1976).